MSc Earth Surface and Water

Department of Earth Sciences

Virus Attachment and Release Processes in Saturated Porous Media under Transient Chemical Conditions

Author:
Andrea Waade

Supervisors:
Prof. Jack F. Schijven
Prof. Dr. Ir. S. Majid Hassanizadeh

August 15, 2013

Acknowledgements

I would like to thank Prof. Jack Schijven for introducing me to the subject of virus transport and for his guidance and encouragement throughout the past year. I would also like to sincerely thank Dr. Gholamreza Sadeghi for his laboratory training and continuous support. Additionally, I would like to thank Prof. Dr. Ir. S. Majid Hassanizadeh and Dr. Thilo Behrends for their guidence and Dr. Amir Raoof for his support with Comsol modeling. A special thank you to my family and close friends for their patience and enthusiasm. A final thanks to the Hydrogeology Group and Utrecht University for the opportunity to conduct my master's research in the Netherlands within the exciting field of Hydrogeology.

Abstract

The effect of pH, ionic strength (IS) and Ca^{2+} on virus transport is known to play a large role in virus removal. This study builds upon recent work by Sadeghi (2012), which studied the effect of hydrochemical conditions on virus fate and transport. Through experimental column studies using bacteriophage PRD1, Sadeghi (2012) found that virus attachment processes could be quantitatively described by changes to IS, pH and Ca^{2+}. However, no correlation between chemical conditions and the coefficient for kinetic detachment were found. In this study, the effect of Ca^{2+} on attachment processes was explored at pH 6, thus expanding on the work of Sadeghi et al. (2012), which was conducted at pH 7. A 3-D sigmoidal relationship was found to relate pH, Ca^{2+} concentration, and sticking efficiency at a constant IS of 10. Additionally, the effect of hydrochemical step-changes in Ca^{2+} and IS were included, with the purpose of quantifying instantaneous step-changes to virus transport processes. Through modeling of the remobilization processes, it was shown that coefficient for kinetic detachment could be modeled as a function of changing IS and Ca^{2+} conditions with respect to time.

Contents

List of Figures

List of Tables

1 Introduction

Groundwater is used as the primary source of drinking water in the majority of countries (Krauss and Griebler, 2011). Aquifers are known to filter contaminants and groundwater is often considered to be a good source for drinking water (Tufenkji et al., 2002). However, groundwater carries a risk of pathogen contamination and in many cases worldwide has been linked with waterborne disease outbreaks (Fong et al., 2007; Gerba, 2004). Thus, an understanding of virus removal properties is of high importance.

The source and fate of viruses in groundwater is a particularly relevant public health concern (Blanc and Nasser, 1996b). Groundwater contamination is often attributed to agricultural infiltration, landfills, leaking septic tanks and urban runoff (Gerba, 2004; Reynolds and Barrett, 2003; Schijven, 2001). Viruses are an important microbiological contaminant for study given that viruses are found in very high concentrations in fecal sources, specifically between 10^5 to 10^{11} infective viruses per gram fecal material (Fong and Lipp, 2005). Additionally, viruses are more infectious and can survive longer in groundwater than most intestinal bacteria (Krauss and Griebler, 2011; Fong and Lipp, 2005; Schijven, 2001). Under normal groundwater temperatures, viruses can remain infectious for several hundred days (Krauss and Griebler, 2011).

Understanding removal processes is not only important from a public health perspective but also in terms of optimizing water re-use strategies. This is especially relevant in countries where there is increased water demand due to urbanization and irrigation water shortages (Meinzen-Dick and Appasamy, 2002). River bank filtration is a type of artificial recharge method which is becoming an increasingly popular for microbial filtration of surface water (Tufenkji et al., 2002; Kuznar and Elimelech, 2007). In the Netherlands, about 14% of drinking water is from artificially recharged surface water (Schijven, 2001).

To assure that drinking water is safe, adequate protection zones of groundwater well systems are required. The distance needed for well protection zones and artificial recharge areas are based upon the travel time of the groundwater (Schijven, 2001). In European countries such as in Austria, Denmark, Germany and the Netherlands, protection zone regulations stipulate that this travel time is between 50 to 60 days (Chave et al., 2006). However, virus removal is known to be dependent on aquifer characteristics and conditions (Schijven and Hassanizadeh, 2000). Thus, knowledge of virus

removal helps further improve protection zone regulations.

Aquifer and groundwater hydrochemical conditions, such as soil and water organic matter level, Ca^{2+} content, ionic strength and pH of groundwater have shown to be important to virus fate and transport (Sadeghi et al., 2013). Hydrochemical conditions should also be seen as part of a dynamic environment. Groundwater is, for example, affected by daily and seasonal weather events and patterns, which can influence groundwater chemical composition, temperature and flow rates (Alley et al., 2002). These changes can occur slowly or instantaneously, as in the case of a high intensity rain event. When there is a change in the chemical composition of the groundwater, attached viruses may be remobilized (Harvey and Ryan, 2004; Sadeghi et al., 2013). Quantitative analysis between hydrochemical conditions and virus groundwater removal allows for improved drinking water quality standards.

1.1 Objectives

This study builds upon recent work by Sadeghi et al. (2012) on the effect of hydrochemical conditions on virus fate and transport. Through experimental column studies using bacteriophage PRD1, Sadeghi et al. (2012) found that virus attachment processes could be quantitatively described by changes in IS, pH and Ca^{2+}. However, no correlation between chemical conditions and the coefficient for kinetic detachment were found. Sadeghi et al. (2012) explored the relationship between Ca^{2+} and attachment processes at a pH of 7. This study further developed these relationships at a pH of 6, using the same experimental methods described by Sadeghi (2012). Additionally, the effect of hydrochemical step-changes were introduced with the purpose of quantifying the effect of pulse hydrochemical changes, which are known to occur in the environment and effect virus transport processes.

The objectives of the study were as follows:

1. To expand the quantitative relationship developed by Sadeghi (2012) between Ca^{2+} and k_{att} at pH 7 and IS of 10 for pH 6, with IS constant.

2. To develop a kinetic transport model which relates transient hydrochemical conditions to detachment and attachment processes.

3. To relate the quantitative results for attachment and detachment to the DLVO theory.

The outline of the study includes a literature review, which introduces the physical, chemical and mathematical theory of virus fate and transport processes. Subsequent chapters include the methodology and results of the six column experiments conducted. A discussion and conclusion follow in the final two chapters, which integrates the findings of Sadeghi (2012) with the current study.

2 Virus Fate and Transport: Literature Review

The processes which affect the fate of viruses in groundwater can be explained by both hydrologic transport behavior and the characteristics of virus removal (Tufenkji, 2007). There are three types of experimental methods used to collect observation data regarding virus removal processes. These include batch, column and field experiments. In batch experiments, the transport terms are neglected. However, it has been shown that analysis of virus parameters in batch experiments are not well translated to columns or field conditions (Sadeghi et al., 2013). Thus, column and field experiments are the most preferred approaches, given that they include both transport and removal processes (Schijven, 2001; Tufenkji, 2007). In field experiments it is easier to simulate the complexity and heterogeneity of the natural environment, whereas in column experiments physiochemical relationships can be better defined and controlled.

Hydrologic transport processes include advection and dispersion. Dispersion contributes to the spreading of viruses due to diffusion processes and inter- and intra-pore velocity heterogeneities. Advection is the transport of viruses due to the average flow velocity. The transport of viruses due to the process of advection and dispersion is found for column and field experiments using a conservative tracer (Yates and Yates, 1991). The advection-dispersion transport equation is shown below for a one dimensional case.

$$\frac{\partial C}{\partial t} = D_x \frac{\partial^2 C}{\partial x^2} - v \frac{\partial C}{\partial x} \tag{1}$$

Dispersion of tracer studies has been shown to accurately simulate the flow of viruses in homogenous grained material (Pieper et al., 1997). However, in aquifers where fractured flow or preferential flow paths exist, breakthrough of micro-organisms may be faster compared to tracers (Harvey, 1997). This is

due to the smaller size of tracer ions, such as bromide and chloride, compared to microorganisms (Harvey, 1997).

2.1 Attachment and Detachment Processes

The fate of viruses is described by the process of inactivation, detachment and attachment (Yates et al., 1987; Schijven and Hassanizadeh, 2000). Attachment and detachment processes are determined by interactions of viruses at the solid-water interface (Tufenkji, 2007). Inactivation is the destruction of viruses through geochemical or biological processes (Yates and Yates, 1991).

The processes of attachment can be described as either irreversible or reversible. When it is irreversible it is assumed that no detachment takes place. Under reversible conditions, both attachment and detachment processes are involved. Under reversible conditions, the rate at which the adsorption process occurs relative to flow velocity is important (Tufenkji, 2007). When attachment is slow relative to the flow velocity, adsorption is considered to be kinetically limited.

Under kinetic attachment, viruses are first transferred from the aqueous phase to the grain surface and then attached to the surface through physical and chemical interactions (Tufenkji, 2007). The rate of attachment depends on which of the aforementioned processes is rate limiting (Schijven, 2001). Kinetic behavior has been shown to be the predominant transport and removal process in columns and at the field scale (Bales et al., 1997; Schijven and Hassanizadeh, 2000). Subsequent detachment can also be described as kinetic. The governing transport equations are as follows (Schijven et al., 2000b),

$$\frac{\partial C}{\partial t} = \frac{\partial}{\partial x}(\alpha_L v \frac{\partial C}{\partial x}) - v\frac{\partial C}{\partial x} - k_{\text{att}}C + k_{\text{det}}\frac{\rho^b}{n}S - n\mu_l C \tag{2}$$

$$\frac{\partial S}{\partial t} = \frac{n}{\rho^b}k_{\text{att}}C - k_{\text{det}}S - \mu_s S \tag{3}$$

where C [pfp L^{-1}] is the number of free viruses in solution, S [pfp M^{-1}] is the number of attached viruses per unit mass of soil, ρ^b [M L^{-3}] is the dry bulk density, α_L [L] is the dispersivity, v [L T^{-1}] is the pore water velocity, n [-] is the porosity, k_{att} and k_{det} [T^{-1}] are the attachment and detachment rate coefficients, respectively, μ_s [T^{-1}] is the inactivation rate coefficients for attached to viruses and μ_l [T^{-1}] is the inactivation rate coefficient for free viruses.

2.2 Inactivation

Inactivation or death of viruses occurs when virus components are damaged and are no longer able to infect host cells (Harvey and Ryan, 2004). Inactivation of viruses occurs to both viruses which are attached and in the bulk phase. However, the inactivation rates may not be the same for these two groups (Schijven, 2001). The inactivation rate for attached particles is very difficult to accurately measure and is often found by fitting breakthrough curves (Harvey and Ryan, 2004). The inactivation rate of free viruses is most often measured directly by calculating the rate of decrease of virus concentration in solution with respect to time.

Modeling of virus inactivation is dependent on the environmental conditions. Virus inactivation is usually modeled using first-order kinetics (Schijven, 2001). However, viruses may be sensitive to numerous factors such as temperature, solution composition, pH, conductivity and turbidity (Pang et al., 1997). Additionally, different subsets of the virus population may experience different degrees of sensitivity to physiochemical conditions (Yates et al., 1987). However, temperature is considered to play the largest role in inactivation (Tufenkji, 2007). The equation for inactivation is described by,

$$\mu_l = \frac{-2.3 \log_{10}(\frac{C}{C_0})}{t} \tag{4}$$

Where C_0 is the initial free virus concentration [pfp L^{-1}], t [T] is the travel time, x is the distance [L] and v is the average pore water velocity [m day^{-1}].

2.3 Colloid Filtration Theory

Colloid filtration theory (CFT) is a commonly used to describe colloid attachment, originally developed by Yao et al. (1971). In the classic clean-bed filtration theory, the removal of colloids is described by a first-order kinetic relationship where the removal of suspended and attached particles is a function of distance (Tufenkji and Elimelech, 2005). In this theory a suspended particle collides with a grain, or collector, through the process of interception, diffusion or sedimentation (Yao et al., 1971). The collision efficiency, α, represents the ratio of collisions between particles and collector soil grains which lead to attachment (Yao et al., 1971) and is described as follows,

$$k_{\text{att}} = \frac{3}{2} \frac{(1-n)}{d_c} v \alpha \eta_0 \tag{5}$$

Here, α is the sticking efficiency (or the collision efficiency), d_c is the grain size diameter and n is the porosity. The single collector contact efficiency, η_0, is found through empirical relationships and is the rate at which colloids colloid with soil grains (Yao et al., 1971). The sticking efficiency is assumed to be independent of hydrodynamic forces, such as advection and dispersion and can be found from fitting experimental breakthrough curves or from values of k_{att} (Bradford et al., 2002; Schijven, 2001; Pieper et al., 1997; Ryan et al., 1999).

The sticking efficiency can be described as the combined effect of attractive and repulsive forces between the colloids and grains. Thus, the sticking efficiency is dependent upon conditions which affect intersurface forces. Tufenkji and Elimelech (2004a) considered the additional influence of hydrodynamic interactions and van der Waals forces. Through experimental research they found these forces to have a significant affect on η_0. The single collector contact efficiency, η_0, can be determined by the following empirical formula (Tufenkji and Elimelech, 2004a),

$$\eta_0 = 2.44 A_s^{1/3} N_R^{-0.081} N_{\text{Pe}}^{-0.715} N_{\text{vdW}}^{-0.052} + 0.55 A_s N_R^{-1.675} N_A^{-0.125} + 0.22 N_R^{-0.24} N_G^{1.11} N_{\text{vdW}}^{-0.053} \tag{6}$$

where A_s is a porosity dependent correction factor from Happels model, N_R is the aspect ratio, N_{Pe} is the Peclet number, N_{vdW} is London-van der Waals attractive forces number, N_A is the attraction number; and N_G is the gravitional number.

Recent studies have shown classical CFT to be most applicable on certain chemical and physical conditions (Tufenkji, 2007; Harvey and Ryan, 2004). Under unfavorable conditions some studies have found classical CFT to overestimate experimental results (Tufenkji and Elimelech, 2004b). This inaccuracy may be due to chemical and charge heterogeneities of collector surfaces (Tufenkji and Elimelech, 2005). Physical characteristics which have been shown to influence sticking efficiency include surface roughness, heterogeneous size distributions, and the non-spherical nature of the collectors (Redman et al., 2001a,b; Bradford et al., 2012).

2.4 Forces Governing Attachment Processes and the DLVO theory

Virus attachment and detachment processes are governed by interactions at the soil-particle interface (Harvey and Ryan, 2004; Schijven and Hassanizadeh, 2000). These interactions are characterized by repulsive and attractive forces. The governing forces are determined by hydrochemical and

physical characteristics of the virus, grain and bulk solution (Harvey and Ryan, 2004).

Electrostatic interactions are one of the primary forces which affect virus-grain interactions. Electrostatic interactions come about due to the charged surfaces of both viruses and minerals. Viruses have a surface charge due to the ionization of amino and carboxyl groups on the protein surface. The protonation and deprotonation of these groups depends upon the pH and ionic strength of the groundwater. The pH value at which the virus has a zero net charge, the isoelectric point (pH_{IEP}), varies with the specific type and strain of virus (Harvey and Ryan, 2004; Schijven and Hassanizadeh, 2000). Soils are also most often negatively charged under normal groundwater conditions (pH 4-9). Positive sites are thought to occur due to micro-level heterogeneity, such as from patches of aluminum, iron and manganese oxides (Schijven, 2001; Ryan and Elimelech, 1996; Loveland et al., 1996).

The Derjaguin-Landau-Verwey-Overbeek (DLVO) theory provides a useful framework for analysis of the forces involved in grain-particle interaction. In the DLVO theory, virus adsorption processes are the result of the combination of double layer interactions and van der Waals forces (Murray and Parks, 1980). The DLVO interaction profile is dependent on the separation distance between the colloid and surface of the collector. When these two interfaces are of like charge, the DLVO energy profile includes an attractive well at small separation distance, also known as the primary minimum, and a shallow attractive well, or the secondary minimum, at a larger separation distance (Figure 1a) (Shen et al., 2008). These two minima are separated by energy barriers due to electrostatic repulsion (Figure 1b). Under favorable conditions where soil-grain surfaces are of opposite charge, the energy profile consists of a deep primary minimum and the two surfaces are attractive at all separation distances (Figure 1b).

Double layer forces are due to excess ions which accumulate along the charged grain surface (Ryan and Elimelech, 1996). The ions along a grain surface attract counterions. These counterions can be bound to the surface (also known as the Stern layer) or remain near the surface in the diffuse electric double-layer (Israelachvili, 2011). Unlike double layer forces, London-van der Waal forces are always attractive and do not depend significantly on bulk solution composition, such as electrolyte concentration and pH (Israelachvili, 2011). London-van der Waal forces are due to the attraction between molecules due to induced dipole moments. When surfaces are similarly charged, the van der Waal forces oppose the double layer forces which

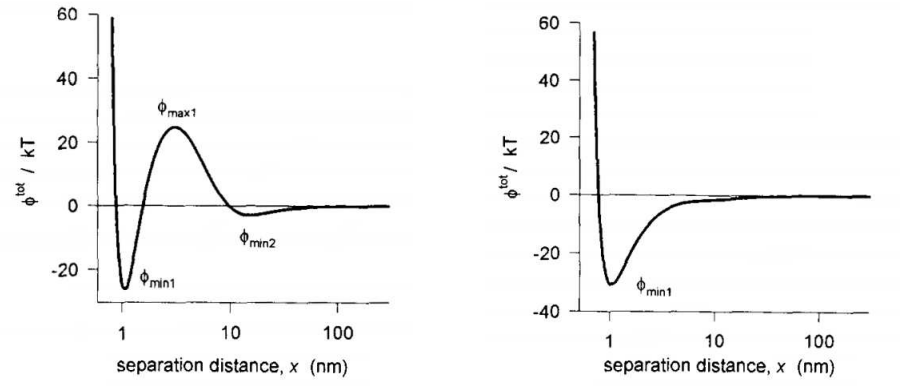

(a) Unfavorable (b) Favorable

Figure 1: The net effect of DLVO forces on potential energy between two charged surfaces under unfavorable (a) and favorable (b) conditions. Figures from Loveland et al. (1996).

are repulsive. The secondary minimum is the result of van der Waal forces overcoming the repulsive double layer forces, given the faster decay of double layer forces with respect to distance (Ryan and Elimelech, 1996). Under favorable conditions both forces act in tandem.

Attachment is directly relatable to the DLVO energy profile. When attachment occurs in the primary minimum it is often considered to be irreversible or very slow (Loveland et al., 1996; Harvey and Ryan, 2004). This is because the energy needed for colloids to overcome primary maximum once attached in the primary minimum is much higher than their average thermal energy (Loveland et al., 1996). When colloids attach in the primary minimum, k_{att} is considered to be inversely related to the height of the energy barrier (Schijven and Hassanizadeh, 2000). The kinetic detachment coefficient describes the process in which diffusion and advection transports viruses from the boundary layer to the bulk solution (Harvey and Ryan, 2004; Schijven, 2001; Bradford et al., 2012). It has been hypothosized that colloid attachment in the secondary minimum is reversible due to the shallow depth of the secondary minimum, which under specific circumstances is comparable to the thermal energy of colloids (Bradford et al., 2012; Loveland et al., 1996).

DLVO interactions can be quantified and related to attachment and detachment processes. This is done through finding the sum of potential energy

with respect to separation distance (x) for the two approaching colloid-grain surfaces.

$$\sigma_{tot}(x) = \sigma_{vdW}(x) + \sigma_{dl}(x) \tag{7}$$

Van der Waal forces are calculated for a specific Hamaker constant (Eq. 8). The Hamaker constant is related to the properties of the interacting surfaces and the medium (Ryan and Elimelech, 1996). To quantify the double layer forces, the Poisson-Boltzman (PB) equation (Eq. 9) is used to determine the potential, ψ, electric field, $\delta\psi/\delta x$, and counterion density, ρ, with respect to the distance between the two surfaces (Israelachvili, 2011). From solutions to the PB equation, the electrostatic interaction of free energy can be determined (Sadeghi, 2012; Israelachvili, 2011).

$$W_{\text{vdw}} = -A/(12\pi x^2) \tag{8}$$

$$\delta^2\psi/\delta x^2 = -(ze\rho_0/\epsilon_0\epsilon)e^{-ze\psi/kt} \tag{9}$$

where z is the valency of the ion [-], x [L] is the distance between the two surfaces, ϵ_0 is the permittivity of free space, ϵ is the permittivity of water and k is the Boltzmanns constant [J K^{-1}]. Analytical solutions to the equation exist given solutions of 1:1 and 1:2 electrolyte solutions (Sadeghi, 2012).

There are additional forces not included in the DLVO theory which may have a significant effect on accurate DLVO predictions (Bradford et al., 2002). These forces include short range forces, such as hydration forces and steric repulsion (Schijven and Hassanizadeh, 2000). The inclusion of these forces has been used in extended DLVO theories and quantitative solutions have been modified to include these forces (Simoni et al., 2000; Hermansson, 1999). However, accurate predictions of the combined electrostatic forces is often complex and simplifications are commonly made, which can potentially limit the accuracy of the predictive findings (Ryan and Elimelech, 1996; Sadeghi, 2012).

Previous studies which have developed quantitative solutions for DLVO forces have found varying results regarding the role of the secondary minimum. These discrepancies are in part related to colloid size; viruses are considered to be between 20-200 nm and colloids have been defined in previous studies to be as large as 20μm (Schijven, 2001; Bradford et al., 2002). For larger colloidal particles, reversible attachment has been directly related to the role of secondary minimum (Kuznar and Elimelech, 2007; Elimelech and O'Melia, 1990a,b; Tufenkji and Elimelech, 2004a, 2005). However, quantitative calculations for viruses have shown that the secondary minimum is not

deep enough to explain observed reversible attachment processes (Loveland et al., 1996; Sadeghi, 2012). Colloid size is important given that electrostatic forces and hydrodynamic torque are functions of the particle size (Bradford et al., 2007; Shen et al., 2008). Additionally, the trapping of larger colloids in pore throats, also known as straining, has been included into recent secondary minima calculations (Bradford et al., 2007).

2.5 Geochemical effects on Attachment and Detachment

The process of attachment and detachment is complex due to the physical and chemical heterogeneity of soil grains. The interactions between the surface grains and viruses depend on virus characteristics, surface charge of aquifer grains and chemistry of the groundwater (Harvey and Ryan, 2004). This section will give a brief introduction to the effect of chemical heterogeneity of aquifer media and solution chemistry on virus transport, followed by a more detailed discussion on the effect of pH, ionic strength and bivalent cations respectively.

Aquifer media is chemically heterogeneous and can contain varying amounts of oxides, clay minerals, organic matter and carbonates (Ryan and Elimelech, 1996). These components affect the surface charge of the aquifer media, which in turn affects colloid-grain interaction energy. Positively charged surfaces, such as oxides, for example, most often make up only small patches on the grain surface but are known to significantly increase virus removal (Ryan and Elimelech, 1996). Given that these patches often have small surface areas, the sites may become filled and thus removal rates may be limited overtime, a condition known as blocking (Schijven, 2001). Comparatively, absorbed organic matter promotes hydrophobic interactions between grains and viruses (Schijven, 2001).

Solution chemistry, which can change with respect to time, has a large effect on virus transport processes. This includes the effect of pH, ionic strength, and dissolved organic matter. Transients in solution chemistry have been shown to effect particle-surface interactions (Grolimund and Borkovec, 2006). When this type of change occurs, the thickness of the electric double layer is affected, which may result in grain-colloid repulsive forces outweighing attractive forces (Bradford et al., 2012; Tosco et al., 2009; Ryan and Elimelech, 1996). In response to perturbations, detachment is no longer only

a diffusive processes but characterized in terms of a large release of viruses (Bradford et al., 2012).

2.6 Effect of pH

The pH of groundwater is important given its effect on the surface charge of both viruses and most minerals (Israelachvili, 2011). Most viruses are negative at a normal groundwater pH levels. Comparatively, most minerals, such as silicates, are also negatively charged at neutral pH. Thus, the higher the pH the more electrostatic repulsion will result between grains and viruses, given that the pH is above the pH_{IEP} value. Consequently, viruses with a higher pH_{IEP} value have a higher attachment rate to negatively charged minerals (Schijven, 2001). Loveland et al. (1996) found that the pH had a large effect on the attachment processes of PRD1, and that the bacteriophage only attached to quartz grains at a pH value of 5 and below. When ferric oxyhydroxide was partially coated on the quartz sand grains, PRD1 attached at pH values of 7.5 and below given the introduction of positive binding sites on the mineral surface.

2.7 Ionic Strength

Ionic strength affects the distance of overlap between aquifer media and electrostatic double layers (Harvey and Ryan, 2004; Ryan and Elimelech, 1996). Low ionic strength results in fewer ions counterbalancing the surface charge of the grains and thus there is a larger extension of double layers into the solution. Similarly, at high ionic strengths there is a double layer compression and a reduction of electrostatic repulsion (Harvey and Ryan, 2004; Israelachvili, 2011). A reduction in ionic strength often occurs in nature due to effects of precipitation, irrigation or artificial recharge (Ryan and Elimelech, 1996). Ionic strength has been shown to have an effect on both attachment and on release processes in experimental studies for viruses (Bales et al., 1993; Sadeghi, 2012). Some studies have also shown a critical decrease in IS concentration is needed for particle release (Lenhart and Saiers, 2003).

2.8 Bivalent Counterions

The role of bivalent ions, such as Ca^{2+}, is important in adsorption processes because of their ability to better shield the surface charge of negatively

charged aquifer grains compared to monovalent ions. Dissolved Ca^{2+} is often found in natural groundwater systems due to the dissolution of limestone.

Given its bivalent charge, Ca^{2+} has a large effect on both surface potential, ψ, and surface charge density, σ, of mineral surfaces. The valency of ions is exponentially related to surface potential, as shown in the PB equation (Eq. 9). Ca^{2+} also specifically binds to both viruses and soil grains, whereas monovalent ions remain in the double layer boundary (Bradford et al., 2012). This binding is often referred to as the ability of bivalent ions to form a cation-bridge (Harvey and Ryan, 2004). Binding will likely reduce ψ and σ even further and consequently reduce the double layer interaction energy (Israelachvili, 2011; Schijven et al., 2000a; Harvey and Ryan, 2004). The affect of binding on surface potential is found quantitatively through the Grahame (1953) equation. Given the large effect of Ca^{2+}, it has been shown that when the divalent ion concentration is larger than 3% of the monovalent concentration the surface potential is only determined by the divalent ion concentration. It has been shown that given the large effect of Ca^{2+} on surface potential, small amounts of Ca^{2+} can fully neutralize the surface of negatively charged minerals (Israelachvili, 2011).

Sadeghi et al. (2012) found a linear relationships between Ca^{2+} concentration and k_{att} and α at a pH of 7 and IS of 10 (Eqs. 10 and 11). These relationships were modeled as linear relationships with an intercept of zero.

$$k_{\text{att}}(h^{-1}) = 0.011[Ca^{2+}] \tag{10}$$

$$\alpha = 0.00026[Ca^{2+}] \tag{11}$$

2.9 Modeling of Remobilization Processes

Detachment is traditionally modeled as a diffusion-controlled process (Harvey and Ryan, 2004; Schijven, 2001). However, it is known that viruses can remobilize in the environment due to chemical perturbations, thus causing a large flux in virus detachment (Bradford et al., 2002). Several recent models have been built to simulate colloid release, primarily with respect to step-changes in ionic strength (Bradford et al., 2012; Lenhart and Saiers, 2003; Grolimund and Borkovec, 2006; Tosco et al., 2009; Bradford et al., 2011a). These models will be further elaborated upon in this section.

Lenhart and Saiers (2003) and Tosco et al. (2009) modeled the relationship between kinetic detachment and remobilization as a discontinuous function. This function was based on a critical IS concentration. Once the critical

concentration was reached, a quick pulse release was induced, which for Tosco et al. (2009) was formulated in terms of the disappearance of the detachment-energy barrier. An assumption of these models is that the release profile does not depend on IS once a critical IS concentration is reached. The coefficients for describing these processes are modeled using empirical relationships that require several fitting parameters.

Grolimund and Borkovec (2006) analyzed both the effect of Ca^{2+} and US, where they relate free virus concentration to the migration of Ca^{2+} and IS solution fronts. The model is described by a first-order release rate coefficient and first-order deposition rate coefficient. The attachment coefficient is assumed to depend on a critical concentration and relationship between monovalent and divalent ions. Although these relationships relate IS and Ca^{2+} to release concentrations, the relationships are fully empirical.

Bradford et al. (2011a, 2012) proposed a model for remobilization processes which was micro-process oriented rather than empirically based. Their model includes two mobile regions for colloid interaction and transport (Figure 2). Region 1 is characterized by relatively high velocity where colloids are transported by advection and dispersion. Region 2 is a low velocity region, which interacts with the soil-water interface (SWI) and region 1.

The mass transfer coefficients were calculated as a function of the secondary minimum energy in the model proposed by Bradford et al. (2012). . The dependency on the secondary minimum is likely insufficient to explain virus transport behavior, which has been shown to have a very shallow secondary minima profile (Sadeghi, 2012; Loveland et al., 1996). Detachment terms used in the model for the solid phase and region 1 include the rate of change in adhesive force and torque due to hydrochemical changes. However, values of torque and force are based on experimental findings of larger colloids rather than viruses (Bradford et al., 2011b). Viruses have not shown the same effect of straining and sedimentation, which are known to influence detachment processes of larger colloids (Bradford et al., 2002). The model also includes a discontinuous step-function with respect to IS concentration, which is based on the assumption that the rate of release is independent of hydrochemical changes.

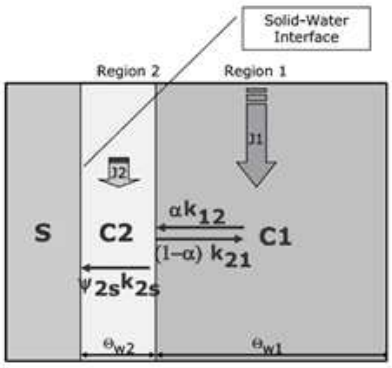

Figure 2: In this figure the relationship between regions 1 and 2 is described by k_{12}, the mass transfer coefficient for colloids from region 1 to 2, k_{21}, the mass transfer coefficient from region 2 to 1, and k_{2s}, the first order colloid immobilization rate coefficient from region 2 to the solid phase. Where C is the colloid concentration in the aqueous phase, J is the colloid flux, w is the volumetric water content, s is the colloid concentration on the solid phase, $2s$ accounts for colloid blocking, and α is the colloid sticking efficiency. Figure from Bradford et al. (2011a).

3 Methodology

3.1 Model Virus: Bacteriophage PRD1

The bacteriophage PRD1 was used in this column study. PRD1 is icosahedra-shaped, 62nm and has an isolectric point between pH 3 and 4 (Harvey and Ryan, 2004). Thus, it is negatively charged under normal groundwater conditions. It was chosen given its functional and structural similarities to adenoviruses and rotaviruses (Sinton et al., 1997; Sadeghi, 2012). Additionally, PRD1 is known to have a low attachment and inactivation rate and thus provides a worst case scenario for virus removal (Blanc and Nasser, 1996a). Given these reasons PRD1 is a commonly used bacteriophage to study virus fate and transport (Harvey and Ryan, 2004).

3.2 Experiments Outline

The column experiments were conducted under steady state flow, saturated conditions and transient chemical conditions. The experimental methodol-

Experiment	Phase 1: Virus Deposition			Phase 2: Release Ca_0			Phase 3: Release IS 1		
	Ca^{2+}	IS	pH	Ca^{2+}	IS	pH	Ca^{2+}	IS	pH
1	0	10	7	-	-	-	0	1	7
2	0	10	6	-	-	-	0	1	6
3	3	10	6	0	10	6	0	1	6
4	1.5	10	6	-	-	-	-	-	6
5	0.5	10	6	0	10	6	0	1	6
6	0.1	10	6	0	10	6	0	1	6

Table 1: Experimental outline of column studies for each of the three phases, where Ca^{2+} and IS are in mM.

ogy was closely adopted from Sadeghi (2012), with slight modifications in experimental design. The experiments included three phases. In phase 1 viruses were introduced to the column for approximately one pore volume at an initial Ca^{2+} concentration (0.1mM-3mM) (Table 1). Phase 2 and 3 comprised of step changes to the chemical composition of the inflow solution. In phase 2, the inflow solution contained zero Ca^{2+} at a constant IS of 10 (when applicable). In phase 3, the inflow solution was switched to a low ionic strength of 1mM and zero Ca^{2+}. The experimental outline is shown in Table 1.

3.3 Column Preparation

The column used for the study had a length of 50 cm and an inner diameter of 5 cm. The glass columns included a top and bottom made of polyoxymethylene and included a hydrophilic polyethylene screen positioned between the lid and column at both the top and bottom. The screens, with a pore size of 80-130 μm, were included to further distribute water over the area of the column. There was an inlet at the bottom for the solution inflow and an inlet in the middle for outflow.

Quartz sand (H31, Sibelcoo, Belgium) was used and had an average grain size of 0.44mm. Columns were packed incrementally under saturated conditions following the procedure described in Sadeghi (2012) and adopted from Foppen et al. (2007). The sand was heated to 850±50 Celcius and then washed in HCl for 48 hours. Prior to adding the sand to the columns, the sand was boiled in de-ionized water in order to saturate the sand and remove gas pockets. Compaction was ensured by tapping the column with a mallet during packing. At the end of each experiment the sand was autoclaved and

new sand was used for the start of each experiment.

New columns were then placed in a temperature-controlled room at 9.5±0.5 degrees Celsius where the experiments were conducted. This temperature was chosen given that it represents normal groundwater temperature in the Netherlands (Sadeghi, 2012). To ensure that there were no remaining impurities, the column was flushed with de-ionized water for several days until the difference in electrical conductivity of the inflow and outflow was less than 10 μs/cm.

3.4 Inflow Solutions

The composition of the inflow solution was calculated using a thermodynamic equilibrium model in MINEQL+ 4.6. The amount of bicarbonate needed to reach pH 6 and 7 at equilibrium with atmospheric pressure was determined. Table 2 outlines the solution composition used with respect to varying calcium concentrations. When the inflow solution wsa prepared it was first allowed to stabilize with the atmosphere. To reach the desired pH following stabilization, small amounts of either NaOH or HCl was added to the solution without significant alteration of the IS. All chemicals were supplied from Merck and were of analytical grade.

Experiment	pH	$NaHCO_3$ (mM)	NaCl (mM)	$CaCl_2$ (mM)	IS (mM)
Ca^{2+} 0	7	0.08	10	0	10
Ca^{2+} 0	6	0.01	10	0	10
Ca^{2+} 10	6	0.01	10	0.1	10
Ca^{2+} 20	6	0.01	8	0.5	10
Ca^{2+} 60	6	0.01	5	1.5	10
Ca^{2+} 120	6	0.01	1	3	10

Table 2: Molar composition of the inflow solutions.

3.5 Experimental Procedure

The column was stabilized to the desired inflow solution until the differences in pH and electrical conductivity of the inflow and outflow were less than 0.05 and 10 μS/cm, respectively. The flow rate of the solution was targeted to be between 62 ml/hr and 64 ml/hr to simulate normal groundwater conditions

in sand. The flow rate was measured prior to seeding and after breakthrough of viruses to ensure consistency.

The seeding suspension was made with a high concentration of PRD1 bacteriophage (between 10^5 and 10^6 plaque forming particles per milliliter [pfp/ml]) and inflow solution. The seeding suspension was added to the column for approximately one pore volume before switching to bacteriophage-free inflow solution. A steady state condition was kept for approximately 20 pore volumes, at which point the first release was initiated by a step-change in inflow solution. This condition was continued for another 20 pore volumes before the second release was initiated (if applicable). A fraction collector was used to continuously collect outflow at 15 minute intervals in 20-ml glass tubes.

3.6 Sample Analysis

The samples were analyzed using the plaque forming technique as defined by ISO 10705-1 (1995) . Nalidixic acid was omitted from the procedure since the host bacteria, Salmonella typhimurium LT-2, is sensitive to nalidixic acid. Given that the samples were assumed to be pure from other bacteria, Nalidixic acid was assumed not to be necessary. PRD1 and Salmonella typhimurium LT-2 were provided by the National Institute of Public Health and the Environment, Bilthoven, The Netherlands (RIVM).

3.7 Concentration Measurements and Procedural Quality Control

The inflow Ca^{2+} concentrations were measured by Optical ICP-OES analyses. Following sample analysis for plaque forming units, sample tubes were analyzed to determine the point of breakthrough in Ca^{2+} concentration. Similarly, electrical conductivity (EC) measurements were taken from sample tubes for releases measuring change in high to low ionic strength.

The virus deposition phase of the first two experiments were previously conducted by Sadeghi (2012). The fitted parameter results, k_{att} and k_{det}, were compared to ensure procedural consistency.

3.8 Inactivation and Parameter Estimation

The bacteriophage seeding suspension solution was sampled for at least 3 months following the end of the experiment. The inactivation rate coefficients, μ_l, was estimated from laboratory measurements and linear regression analysis. The pore water velocity was calculated from the measured flow water velocity of the column. Dispersivity and porosity of the column were previously calculated by the procedure outlined by Sadeghi (2012), using a conservative tracer in the column.

3.9 Modeling

3.9.1 Phase 1: Virus Deposition

The experimental breakthrough curves were modeled in Hydrus 1-D (4.1.4) and COMSOL Multiphysics (4.3.1.161). The models were generated under one-dimensional steady state flow and fully saturated conditions. The following boundary conditions were included,

$$C = C_0 \text{ at } x = 0 \text{ and } \frac{\delta C}{\delta x} = 0 \text{ at } x = L \text{ ,where } L \text{ is the column length.}$$

The results of the initial breakthrough curve for each experiment were simulated using Hydrus 1-D, where k_{att} and k_{det} were fitted. The relationship between k_{att} and Ca^{2+} at a pH of 6 was developed through 2-D surface fitting using the pyeq2 Python library. The pyeq2 Python library was also used for the development of a 3-D model for relationship between sticking efficiency, pH and Ca^{2+}.

3.9.2 Phase 2 and 3: Virus Remobilization

COMSOL Multiphysics was used to simulate k_{att} and k_{det} for the combined three phases. The COMSOL Transport of Diluted Species package was used. The general equations (Eqs. 2 and 3) were included in model to simulate the sorbed virus mass and free virus concentrations. The transport of Ca^{2+} and Na^{+} were also modeled, with the assumption that their transport was governed by dispersion and advective flow. The relationship developed for k_{att}, with respect to Ca^{2+} and pH at 6 in Hydrus 1-D, was included in the COMSOL model. For experiments conducted at pH of 7, the relationship developed by Sadeghi (2012) was used (Eq. 10).

The coefficient for k_{det} was determined as a function of the change in respective hydrochemical inflow solutions. It was hypothesized that the release rate coefficient was dependent on outflow IS and Ca^{2+} conditions. It was tested whether there was a direct correlation with outflow IS and Ca^{2+} concentration, or whether the first or second derivative could describe the virus concentration breakthrough profiles. The first and second derviatives of IS and Ca^{2+} outflow concentrations were determined using R and included as model parameters. The parameter μ_s was also through model simulations.

4 Results

4.1 Phase 1: Virus Deposition

The virus deposition breakthrough curves under varying concentrations of Ca^{2+} and pH 6 at an IS 10 are given in Figure 3. The values fitted in Hydrus 1-D are given in Table 3. The quality control breakthrough curves in experiment 1 and 2 were found to correspond closely with the findings of Sadeghi (2012). The results show that k_{att} remained relatively constant for Ca^{2+} values between 0.5 and 3 mM given pH 6 and IS 10 (Table 3). Values for k_{det} were not found to correlate with respect to Ca^{2+}.

Experiment	Ca^{2+} (mM)	pH	k_{att} (hr^{-1})	k_{det} (hr^{-1})	SSQ	α
1	0	7	0.144 ±0.0559	0.001 ±0.00079	0.81	0.0034
2	0	6	0.0719 ±0.403	0.002 ±0.00019	0.86	0.0017
3	3	6	1.42 ±0.0303	0.005 ±6.5E-05	0.95	0.034
4	1.5	6	1.31 ±0.0123	0.008 ±0.00112	0.78	0.032
5	0.5	6	1.49 ±0.00941	0.002 ±0.00069	0.85	0.035
6	0.1	6	1.23 ±0.0088	0.001 ±0.00081	0.89	0.029

Table 3: Parameter values k_{att}, k_{det} and sticking efficiency for PRD1 breakthrough curves at constant IS 10.

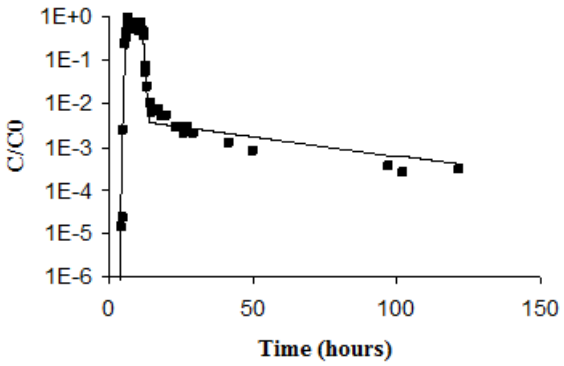

(a) Exp. 1 (pH 7, Ca^{2+} 0 mM, IS 10)

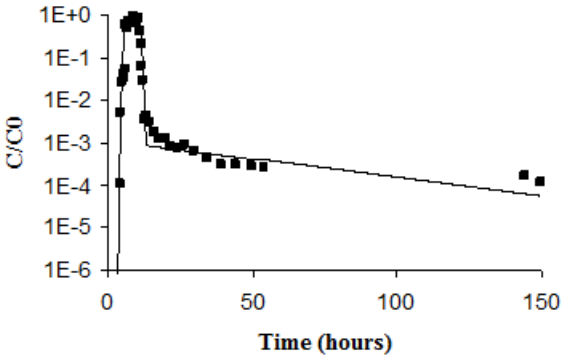

(b) Exp. 2 (pH 6, Ca^{2+} 0 mM, IS 10)

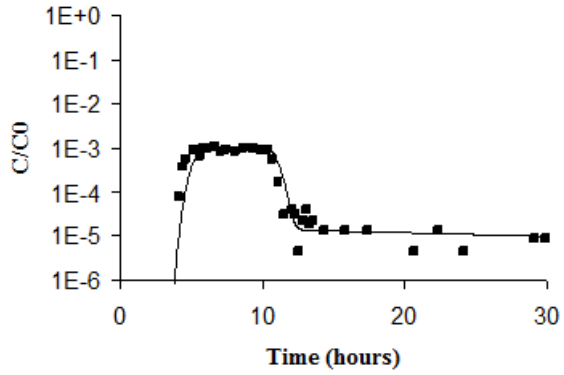

(c) Exp. 3 (pH 6, Ca^{2+} 3 mM, IS 10)

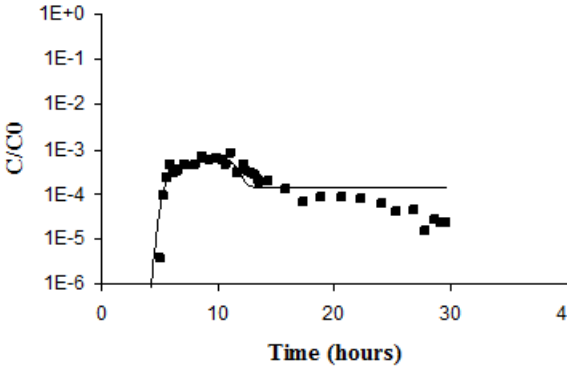

(d) Exp. 4 (pH 6, Ca^{2+} 1.5 mM, IS 10)

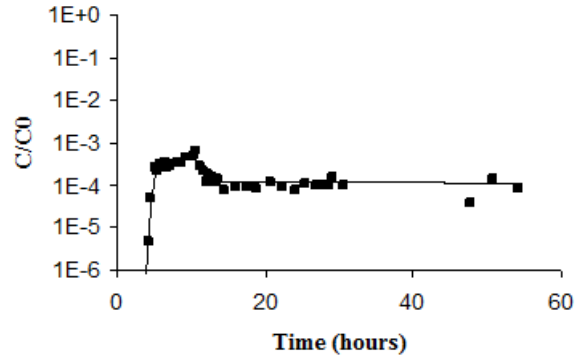

(e) Exp. 5 (pH 6, Ca^{2+} 0.5 mM, IS 10)

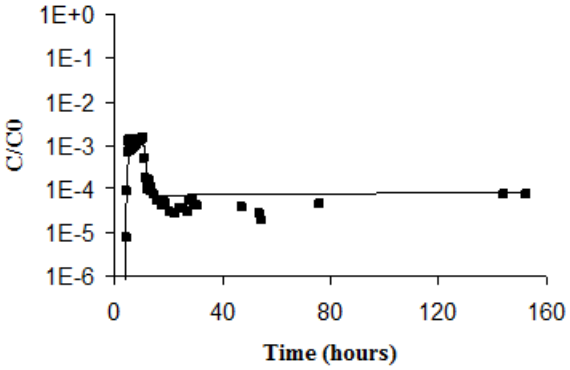

(f) Exp. 6 (pH 6, Ca^{2+} 0.1 mM, IS 10)

Figure 3: PRD1 breakthrough curves modeled as 1-site kinetic in Hydrus 1D. Dots are the observed points and the line indicates the modeled fit.

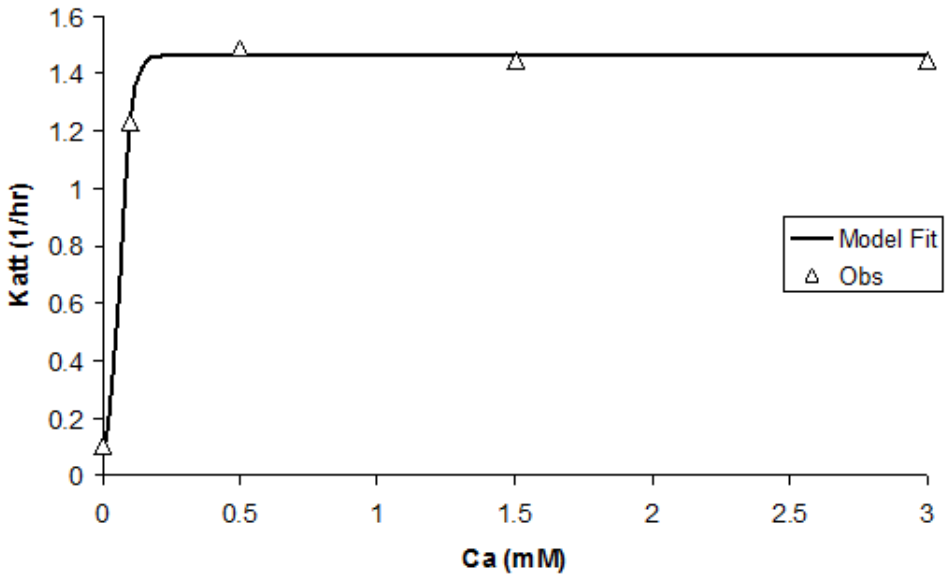

Figure 4: Relationship between Ca^{2+} and k_{att} at a pH of 6 and ionic strength of 10.

The relationship between Ca^{2+} and attachment at pH 6 was found to fit the following sigmoidal relationship with an R^2 of 0.99,

$$k_{att}|_{pH=6} = \frac{1.46}{1 + \exp\frac{0.0639 - Ca^{2+}}{0.0217}} \tag{12}$$

Where Ca^{2+} concentration is in mM. The sigmoidal fit plateaus at a k_{att} of 1.46 [hr^{-1}] and crosses the y-axis at a k_{att} of 0.074 [hr^{-1}](Figure 4). The additional value at zero Ca^{2+} was included from the work of Sadeghi (2012).

4.2 Phase 2 and 3: Virus Remobilization

Following step-changes in inflow solution in phase 2 and 3 there was a pulse remobilization of viruses. The outflow concentrations of IS and Ca^{2+} were found to correlate with the timing and shape of $\frac{\delta[Ca^{2+}]}{\delta t}$ and $\frac{\delta(IS[Na^{+}])}{\delta t}$ (Figure 5). The rate of change of both IS and Ca^{2+} in the outflow is fast and characterized by an upwards spike (Figure 5). The second derivative of IS and Ca^{2+} concentrations in the outflow was not shown to correlate well with

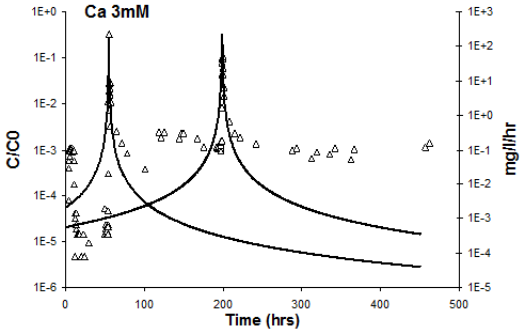

(a) Ca^{2+} 3 mM, pH 6

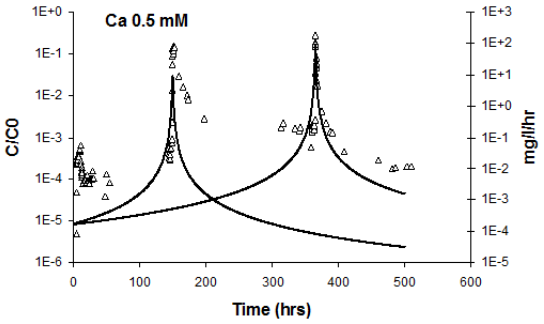

(b) Ca^{2+} 0.5 mM, pH 6

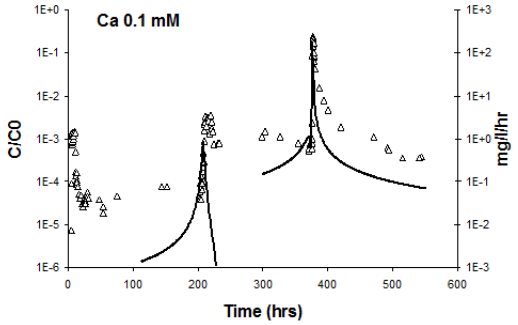

(c) Ca^{2+} 0.1 mM, pH 6

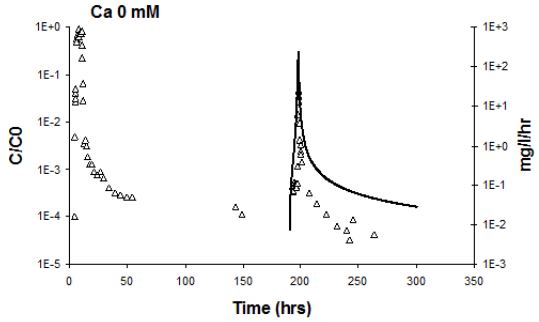

(d) Ca^{2+} 0 mM, pH 6

Figure 5: The rate of change of Ca^{2+} and IS (mg/l/t) related to remobilized virus concentration for experiments conducted at a pH of 6.

the virus concentration profile. The timing of the virus concentration relative to measured concentrations of Ca^{2+} and IS in the outflow are included in Appendix A.

The model developed in COMSOL Multiphysics included the equations developed for k_{att} with respect to Ca^{2+}, for respective pH conditions (Eqs. 10 and 12). The k_{det} coefficient was modeled with respect to $\frac{\delta[Ca^{2+}]}{\delta t}$ and $\frac{\delta(IS[Na^{+}])}{\delta t}$. It was found that following the pulse remobilization period the steady tailing of the releases could be modeled using the constant detachment term (13). Given a constant detachment term, the kinetic detachment coefficient was found to fit the following form,

$$k_{\text{det}}(hr^{-1}) = k_{det,0} - b\frac{\delta[Ca^{2+}]}{\delta t} - c\frac{\delta(IS[Na^{+}])}{\delta t} \tag{13}$$

Where $k_{det,0}$ [T^{-1}] is the constant kinetic detachment coefficient and b and c [V M^{-1} T^{-1}] are remobilization coefficients.

Experiment	$k_{det,0}$ (hr^{-1})	b (L $mg^{-1}hr^{-1}$)	c (L $mg^{-1}hr^{-1}$)	μ_s (hr^{-1})	μ_l (hr^{-1})
0 (pH 7)	0.0003	-	0.005	0.005	0.0025
0	0.0003	-	0.005	0.004	0.003
0.1 (4 mg/L)	0.0003	0.007	0.005	0.001	0.0010
0.5 (20 mg/L)	0.0003	0.007	0.005	0.001	0.0017
3 (120 mg/L)	0.0003	0.0008	0.005	0.001	0.0038

Table 4: Constant detachment coefficient $k_{det,0}$ and remobilization coefficients b and c with respect to initial inflow Ca^{2+} solution.

The change in Na^+ concentration was only included in the second release and modeled as a function of changing IS. Despite small deviations in k_{det} modeled in Hydrus 1-D, a constant value of 0.003 [hr^{-1}] provided a good fit for all experiments (Table 4, (Fig. 6)). The remobilization coefficient, b, was found to have high variability with respect to initial Ca^{2+} concentrations. It was found that coefficient c could be fitted to a constant value of 0.005 (l $mg^{-1}hr^{-1}$) (Table 4).

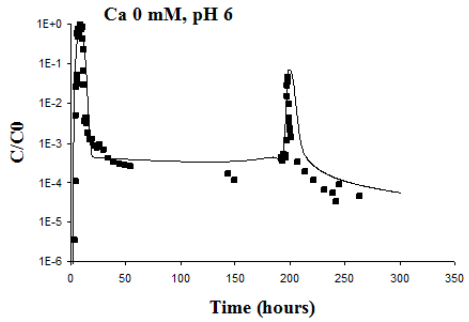

(a) Ca^{2+} 0 mM, pH 6

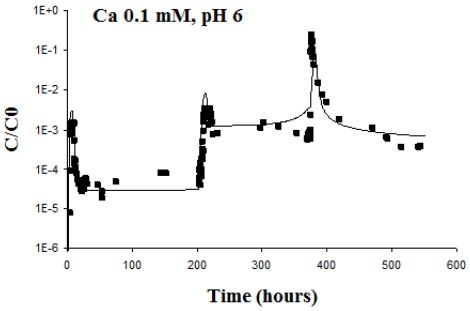

(b) Ca^{2+} 0.1 mM, pH 6

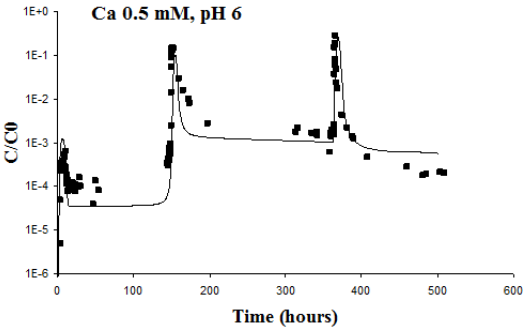

(c) Ca^{2+} 0.5 mM, pH 6

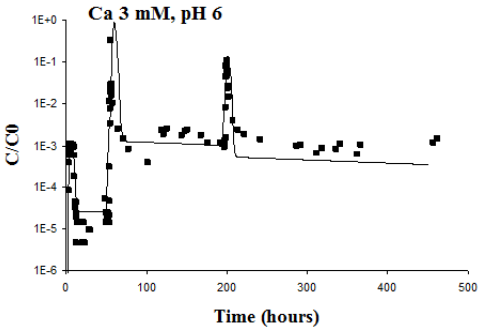

(d) Ca^{2+} 3 mM, pH 6

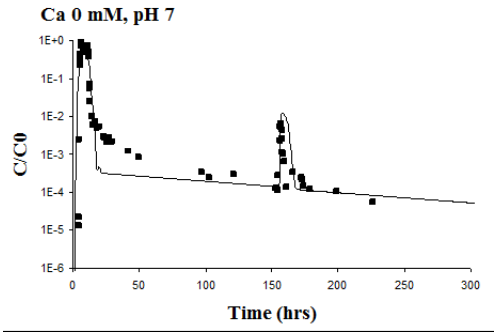

(e) Ca^{2+} 0 mM, pH 7

Figure 6: Normalized observed and modeled virus concentration with initial Ca^{2+} concentrations of 0, 0.1, 0.5 and 3 mM at ionic strength 10. The first release is in response to a step-change to no Ca^{2+} and constant ionic strength. The second release, or first for the experiments with no Ca^{2+}, follows a step-change to IS 1.

5 Discussion

5.1 Effect of Ca^{2+} on k_{att}

Fig. 7 shows the combined results of the current study with the results of Sadeghi (2012). At pH 6, values of k_{att} with respect to Ca^{2+} concentrations are generally larger compared to the results of Sadeghi et al. (2012) at pH 7 (Fig. 7). This finding follows the expectation that with lower pH there is an increase in k_{att}, given the reduction in negative charge density at lower pH (Harvey and Ryan, 2004). Previous studies with PRD1 have also confirmed that lowering pH increases k_{att} (Loveland et al., 1996; Sadeghi et al., 2012). However, the sigmoidal relationship between k_{att} and Ca^{2+} at pH 6 is in contrast to the linear relationship at pH 7 found by Sadeghi (2012).

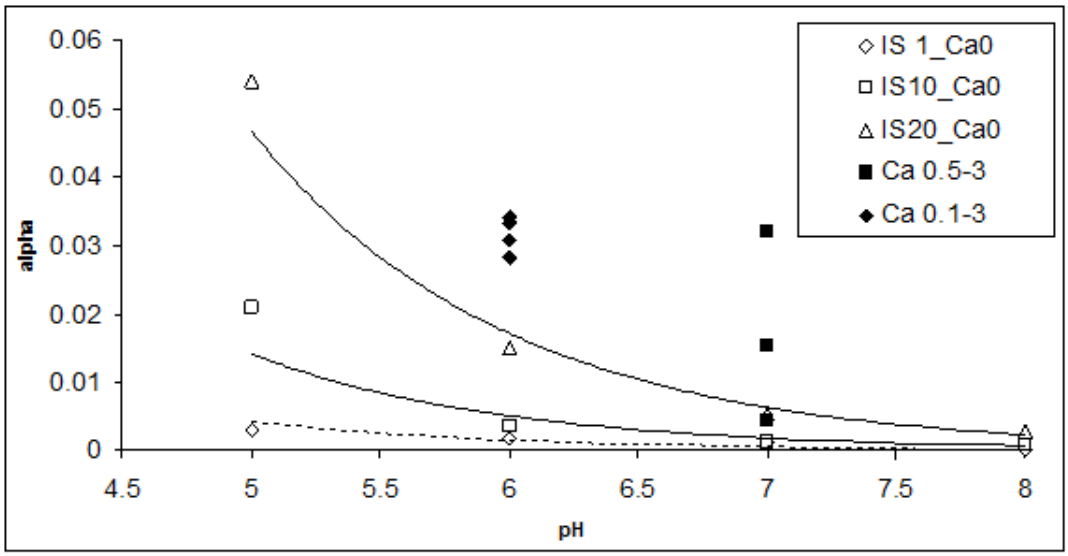

Figure 7: Relationship between sticking efficiency and pH for different IS and Ca^{2+} concentrations (mM). Figure includes data from Sadeghi (2012).

The effect of Ca^{2+} on surface charge density and surface potential is non-linear in accordance to the Poisson-Boltzman equation (Eq. 9). This relationship may indicate why there is a non-linear relationship between k_{att} and Ca^{2+} at pH 6. This also raises the point of whether the relationship between k_{att} and Ca^{2+} at pH 7 would also be sigmoidal if additional experiments were conducted, especially at higher Ca^{2+} concentrations. The

approximate plateau value of k_{att} is 1.46 [hr^{-1}] at pH 6, which slightly larger than the max k_{att} found at pH 7, which was found to be 1.35 [hr^{-1}] at a Ca^{2+} concentration of 3mM. Thus, if a plateu value was found at pH 7 it would be reached later than at pH 6. At a Ca^{2+} concentration of 3mM the IS is almost entirely determined by Ca^{2+} and therefore a plateau could only be observed between 3mM and approximately 3.5 mM at IS 10.

A sigmoidal fit was generated in Python using both the results of the current study and the results of Sadeghi (2012) at a constant IS of 10, with an R^2 value of 94% (Eq. 14). The sigmoidal relationship gives the product of two general logistic equations, where Ca^{2+} is in mM.

$$\alpha = \frac{0.0343}{(1 + e^{-27.76+4.38\text{pH}+4.95\text{Ca}^{2+}-0.96\text{Ca}^{2+}\text{pH}})(1 + e^{0.53-260.3\text{Ca}^{2+}})} \tag{14}$$

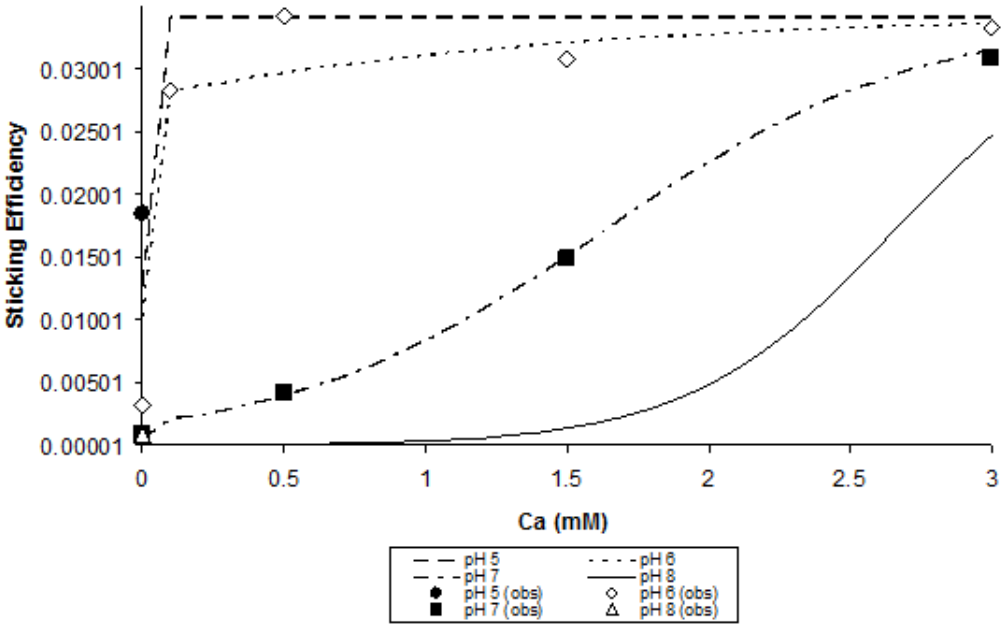

Figure 8: 3-D model of $\alpha\,([Ca^{2+}], \text{pH})$ for pH 5-8, with the inclusion of observation points.

Equation 14 assumes that the relationship between Ca^{2+} and sticking efficiency is sigmoidal at all pH levels (Fig. 8). Given that a higher k_{att} of

2.08 [hr^{-1}] was found at pH 5 by Sadeghi (2012), the height of the plateau was fitted such that it was specific to each pH value. Further experiments with respect to different pH levels are needed to observe whether this plateau effect is also observed at lower pH ranges. It would also be relevant to find whether sticking efficiency is sensitive to Ca^{2+} at higher pH ranges, such as at pH 8.

The plateau in k_{att} with increased Ca^{2+} was not expected. It has been shown in previous studies that k_{att} increases with a decrease in the energy barrier to detachment (Ryan and Elimelech, 1996; Schijven and Hassanizadeh, 2000). Thus, this plateau may indicate that above a Ca^{2+} concentration of approximately 0.5 mM there is no effect on the height of the energy barrier. These results could also be potentially explained by the effect of surface charge at lower pH. Given that the functional groups on the sand grain surface continuously exchange protons and anions with the bulk phase, the pH plays a large role in the attraction of Ca^{2+} to the quartz surface. It could be hypothesized that at a lower pH there is a saturation point of functional groups for Ca^{2+} to bind which gives rise to a plateau.

In the study by Sadeghi (2012) it was shown that the value of the secondary minima was ten times smaller than the 1kt. Additionally, the lack of dependence of Ca^{2+} on constant k_{det} observed in this study and Sadeghi (2012) indicates that the effect of Ca^{2+} k_{att} is not likely described by the role of the secondary minimum.

5.2 Virus Remobilization

The objective of the remobilization experiments was to determine if a kinetic transport model could be applied with respect to changing hydrochemical conditions. The model developed was based on the chemical concentration of the aqueous phase, and thus the model can be described as a macro-process model. The proposed equation accounts for chemical inflow perturbations by taking the derivative of the changing outflow concentrations. Given periods of perturbation, the remobilization term plays the most important role as the constant detachment term is too small to have a measureable effect. A critical value of deposition was not tested given that one step-change was included for IS and Ca^{2+} in each of the experiments (Grolimund and Borkovec, 2006; Bradford et al., 2012). Incremental decreases in IS and Ca^{2+} need to be conductuded to test this hypothesis further for PRD1.

5.2.1 Constant Detachment

The tailing of all breakthrough curves within each experiment could be modeled using a single constant detachment coefficient (Table 4, Eq. 13). This constant term implies that the tailing does not change following changes to IS or Ca^{2+}. The constant detachment term is sensitive to fitted values of μ_s. The fitted values of μ_s remained in the range found in previous literature for PRD1 (Schijven, 2001). Additionally, the ratio of μ_s relative to μ_i was similar to previous studies for PRD1 (Schijven, 2001).

The finding that $k_{det,0}$ was not noticeably affected by hydrochemical conditions, including ionic strength, Ca^{2+} and pH, is supported by previous literature. In the work of Sadeghi (2012) it was found that constant k_{det} did not noticeably change with respect to these hydrochemical conditions. Loveland et al. (1996) explained the process of reversible attachment, given a shallow secondary minimum, was due to virus accumulation at the boundary layer in front of the energy barrier. If this explanation is extended to the effect of changes to IS and Ca^{2+}, $k_{det,0}$ would only be governed by diffusion and not a change in the height of the energy maximum. Compartively, k_{att} would be a function of the height of the energy maximum and hydrochemical changes, which corresponds to the findings of this study at by Sadeghi et al. (2012).

5.2.2 Pulse Remobilization

The release profile differs from the virus deposition profile in that the free virus concentration spike is nearly instantaneous before dropping back to a slow tailing. This spike was found to correlate with the rate of change of Ca^{2+} and IS concentration fronts. The relationship between these fronts during periods of remobilization is in contrast to models which have described release in terms of a discontinuous step-function (Lenhart and Saiers, 2003; Tosco et al., 2009). The simplified approach presented in this macro-process model provides insight to virus release characteristics under transient hydrochemical conditions.

Coefficient c describes the effect of the step-change in IS from 10 to 1 on virus concentration. The magnitude of the remobilization coefficient c was found to be constant for all experiments (Table 4). The finding that c was constant between experiments indicates that there is no dependence of remobilization on previous conditions.

Coefficient b is correlated to the effect of a step-change in Ca^{2+} concentration. The maximum height reached by the remobilization term $b\frac{\delta[Ca^{2+}]}{\delta t}$ followw a non-linear trend for the three experiments (Figure 9). This finding supports previous literature, which indicates that the virus concentration during the pulse period is correlated to the magnitude of the step-change (Bradford et al., 2012). Coefficient b was found to be constant for experiments at 0.1mM and 0.5 mM. This is due to the fact that at 0.1 mM the maximum concentration reached was lower (Figure 6). The results of the current study indicate that the effect of chemical step-change on adhesive forces for retained viruses may not be linearly correlated with the magnitude of the hydrochemical step-change. This finding may apply particularly to the case in which k_{att} similarly follows a non-linear trend with respect to hydrochemical differences in the inflow solution.

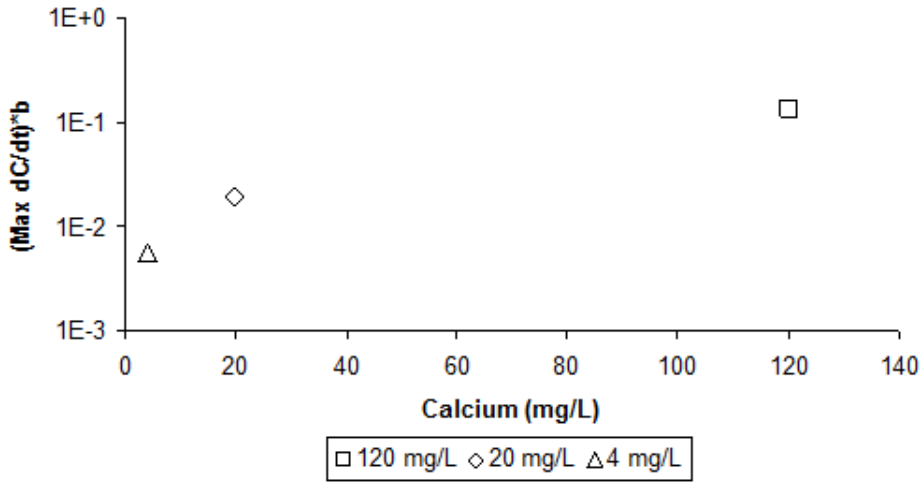

Figure 9: Relationship between the max height reached by the remobilization term for changing Ca^{2+} conditions with respect to Ca^{2+} concentration (mg/L).

Previous studies have found a critical value of hydrochemical change for remobilization to occur (Lenhart and Saiers, 2003). The theory behind a critical release value is that there is an adhesion force which must be overcome for colloids to be released (Bradford et al., 2012). This hypothesis needs to be explored further for viruses, which may not be affected by secondary minima and by the effect of straining. A critical release value could also be explored

in terms of a minimum amount of change needed for release, rather than a critical lower bound value. A potential area of future study is whether small perturbations at the low concentrations could also affect the amount which is released. This could potentially help explain the low maximum height of release found for 0.1 mM relative to 0.5 mM.

The period of fast release associated with the pulse remobilization period is often correlated to the effect of the secondary minima (Bradford et al., 2012, 2011a). However, this implies that k_{att} is not affected by hydrologic effects since it is based on diffusion into the secondary minima. Thus, only k_{det} would depend on changes to the hydrochemical conditions, given that related to the depth of the secondary minima (Sadeghi, 2012). This implication is the opposite of what was found in this study, namely that only k_{att} depends on hydrochemical conditions. The results of this study show that it may be beneficial to study pulse remobilization as continuously related to the change in interaction forces which occur under transient chemical conditions. Given the quantitative findings of Loveland et al. (1996) and Sadeghi (2012) it appears premature to construct a micro-process based on the effect of the secondary minima for virus transport, as has been created for larger colloids (Bradford et al., 2012, 2011a).

5.2.3 Rate of Concentration Change with Time

The macro-process model proposed in this study is dependent on the duration of the hydrochemical perturbation. The length of time over which chemical change occurs should be explored further in future studies. The results of two previous studies are included in this discussion. In these studies the effect on colloids when changes in chemical composition occurred more gradually was explored (Grolimund and Borkovec, 2006; Chu et al., 2000).

In a study by Grolimund and Borkovec (2006) the remobilization period occurs as Ca^{2+} levels slowly decreases and a sharp drop in Na^{+} is induced (Figure 10). The study was conducted for several different homogenous soils using different sized spherical colloids. The results indicate that the slow rate of decrease in Ca^{2+} correlates with the rate of change colloid concentration. This also implies that the rate of change of Ca^{2+} and IS may play varying roles of importance on virus concentration behavior.

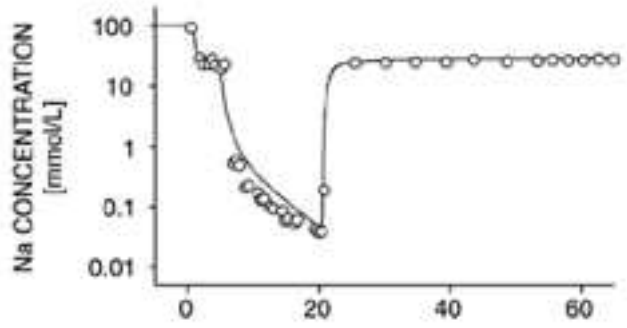

(a) Na^+ Concentration

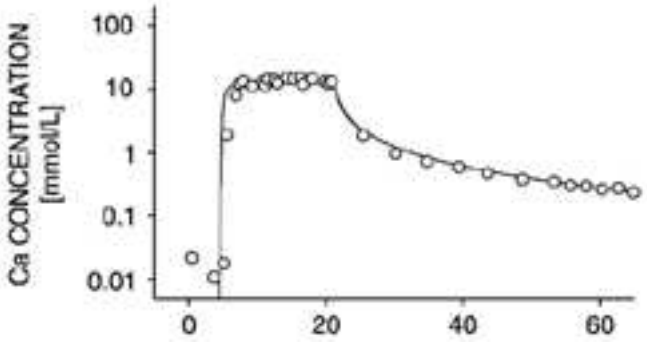

(b) Ca^{2+} Concentration

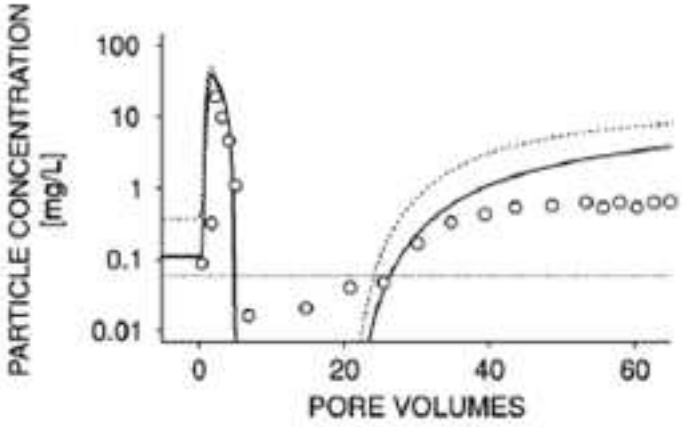

(c) Colloid Concentration

Figure 10: The figure shows changing Na^+ concentration (a), changing Ca^{2+} concentration (b) and colloid concentration (c). The dashed horizontal line in the bottom left is the line for accurate observation and the two curved lines represent different fitting simulations. Figure from Grolimund and Borkovec (2006)

.

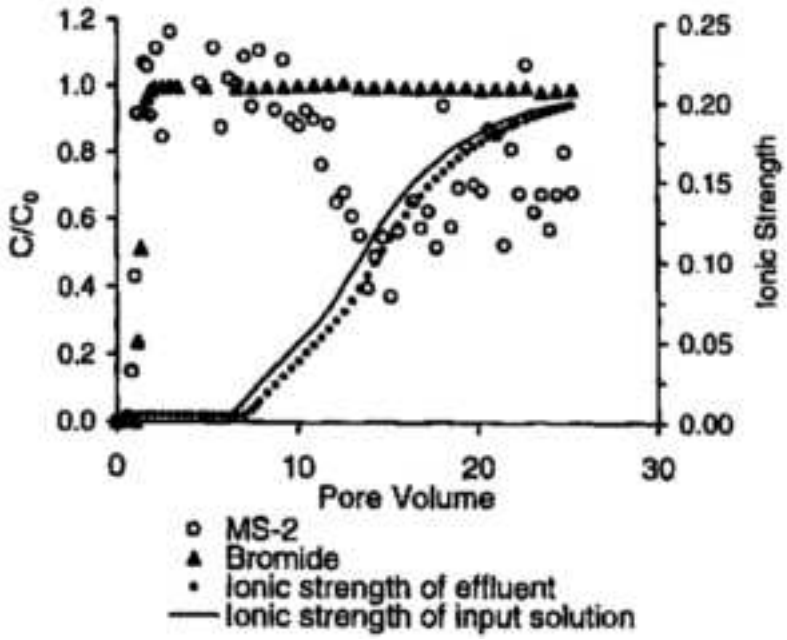

Figure 11: The effect of slowly increasing ionic strength on MS2 concentration. Figure taken from Chu et al. (2000)

In a study by Chu et al. (2000) the effect of slowly increasing IS resulted in a slow decrease in MS2, a conservative bacteriophage (Figure 11). However, the effect of a step increase rather than decrease in IS is not known to have been studied previously. Thus, the implications of this slow rate of change are only speculative. Further studies should include the effect of changing time with respect to both Ca^{2+} and IS. Additionally, the effect of quick perturbations with respect to either Ca^{2+} and IS while inducing a slow perturbation of either IS or Ca^{2+}, respectively, should also be explored.

5.3 Conclusions

The objective of the study was to quantitatively determine the effect of hydrochemical conditions, including Ca^{2+}, pH and ionic strength, on virus attachment and detachment processes in the subsurface. The work of Sadeghi (2012) was expanded to include the effect of pH on the relationship between Ca^{2+} and attachment rate coefficients. A 3-D model was created to simulate the relationship between k_{att}, pH and Ca^{2+} at a constant IS of 10.

The study included the effect of virus remobilization during step-changes to IS and Ca^{2+}. To simulate transient hydrochemical conditions on virus remobilization, a macro-process transport model was developed. Quantitative analysis regarding the effect of transient hydrochemical conditions on virus transport can help guide drinking water protection zone regulations.

References

Alley, W. M., Healy, R. W., Labaugh, J. W., and Reilly, T. E. (2002). Flow and storage in groundwater systems. *Science*, 296:1985–1990.

Bales, R., Li, S., Maguire, K., Yahya, M., , and Gerba, C. (1993). MS-2 and poliovirus transport in porous media: Hydrophobic effects and chemical perturbations. *Water Resources Research*, 29:957–963.

Bales, R. C., Li, S., Yeh, T. C. J., Lenczewski, M. E., and Gerba, C. P. (1997). Bacteriophage and microsphere transport in saturated porous media: Forced-gradient experiment at Borden, Ontario. *Water Resources Research*, 33(4):639–648.

Blanc, R. and Nasser, A. (1996a). Effect of effluent quality and temperature on the persistence of viruses in soil. *Water Science and Technology*, 33:237–242.

Blanc, R. and Nasser, A. (1996b). Human enteric viruses in groundwater from a confined bedrock aquifer. *Environmental Science & technology*, 41:6606–6612.

Bradford, S. A., Torkzaban, S., Kim, H., and Simunek, J. (2012). Modeling colloid and microorganism transport and release with transients in solution ionic strength. *Water Resources Research*, 48(9):W09509.

Bradford, S. A., Torkzaban, S., and Simunek, J. (2011a). Modeling colloid transport and retention in saturated porous media under unfavorable attachment conditions. *Water Resources Research*, 47(10):W10503.

Bradford, S. A., Torkzaban, S., and Walker, S. L. (2007). Coupling of physical and chemical mechanisms of colloid straining in saturated porous media. *Water Research*, 41(13):3012–3024.

Bradford, S. A., Torkzaban, S., and Wiegmann, A. (2011b). Pore-scale simulations to determine the applied hydrodynamic torque and colloid immobilization. *Vadose Zone Journal*, 10(1):252–261.

Bradford, S. A., Yates, S. R., Bettahar, M., and Simunek, J. (2002). Physical factors affecting the transport and fate of colloids in saturated porous media. *Water Resources Research*, 38(12):63–1.

Chave, P., Howard, G., Schijven, J., Appleyard, S., Fladerer, F., and Schimon, W. (2006). Protecting groundwater for health – Managing the quality of drinking water sources. *IWA Publishing*, pages 465–492.

Chu, Y., Jin, Y., and Yates, M. V. (2000). Virus transport through saturated sand columns as affected by different buffer solutions. *Journal of Environmental Quality*, 29(4):1103–1110.

Elimelech, M. and O'Melia, C. R. (1990a). Effect of particle size on collision efficiency in the deposition of brownian particles with electrostatic energy barriers. *Langmuir*, 6(6):1153–1163.

Elimelech, M. and O'Melia, C. R. (1990b). Kinetics of deposition of colloidal particles in porous media. *Environmental science & technology*, 24(10):1528–1536.

Fong, T. and Lipp, E. (2005). Enteric viruses of humans and animals in aquatic environments: Health risks, detection, and potential water quality assessment tools. *Microbiology and Molecular Biology Reviews*, 69:357–371.

Fong, T., Mansfield, L., Wilson, D., Schwab, D., Molloy, S., and Rose, J. (2007). Massive microbiological groundwater contamination associated with a waterborne outbreak in Lake Erie, South Bass Island, Ohio. *Environmental Health Perspectives*, 115.

Foppen, J., van Herwerden, M., and Schijven, J. (2007). Transport of Escherichia coli in saturated porous media: Dual mode deposition and intrapopulation heterogeneity. *Water Research*, 41(8):1743–1753.

Gerba, C. (2004). Why the concern about pathogens in water? *Southwest Hydrology - The Resource for Semi-Arid Hydrology*, 3(6):14–15.

Grahame, D. C. (1953). Diffuse double layer theory for electrolytes of unsymmetrical valence types. *The Journal of Chemical Physics*, 21:1054.

Grolimund, D. and Borkovec, M. (2006). Release of colloidal particles in natural porous media by monovalent and divalent cations. *Journal of contaminant hydrology*, 87(3):155–175.

Harvey, R. and Ryan, J. (2004). Use of prd1 bacteriophage in groundwater viral transport, inactivation and attachment studies. *FEMS Microbiology Ecology*, 49:3–16.

Harvey, R. W. (1997). Microorganisms as tracers in groundwater injection and recovery experiments: a review. *FEMS Microbiology Reviews*, 20:461–472.

Hermansson, M. (1999). The dlvo theory in microbial adhesion. *Colloids and Surfaces B: Biointerfaces*, 14(1):105–119.

ISO (1995). *ISO 10705-1 – Water Quality – Part 1 – Detection and Enumeration of Bacteriophages: Enumeration of F-specific RNA bacteriophages.* International Organization for Standardization, Geneva, Switzerland.

Israelachvili, J. N. (2011). *Intermolecular and surface forces: revised third edition.* Academic press.

Krauss, S. and Griebler, C. (2011). Pathogenic microorganisms and viruses in groundwater. Technical Report 6, Acatech Materialien, Munich, Germany.

Kuznar, Z. and Elimelech, M. (2007). Direct microscopic observation of particle deposition in porous media: Role of secondary energy minimum. *Colloids and Surfaces*, 107:1–56.

Lenhart, J. J. and Saiers, J. E. (2003). Colloid mobilization in water–saturated porous media under transient chemical conditions. *Environmental Science & Technology*, 37(12):2780–2787.

Loveland, J., Ryan, J., Amy, G., and Harvey, R. (1996). The reversibility of virus attachment to mineral surfaces. *Colloids and Surfaces A: Physicochemical and Engineering Aspects*, 107:205–221.

Meinzen-Dick, R. and Appasamy, P. P. (2002). Urbanization and intersectoral competition for water. Technical report, Woodrow Wilson International Centre for Scholars. Environmental Change and Security Project, Washington, DC. In Finding the source. The linkages between population and water.

Murray, J. P. and Parks, G. (1980). Poliovirus adsorption on oxide surfaces. *Particulates in Water*, 89:97–133.

Pang, L., Close, M., Goltz, M., Noonan, M., and Sinton, L. (1997). Filtration and transport of Bacillus subtilis spores and the FRNA phage MS2 in a coarse alluvial gravel aquifer: Implications in the estimation of setback distances. *Journal of Contaminant Hydrology*, 77(3):165–194.

Pieper, A., Ryan, J., Harvey, W., Amy, G., Illangasekare, T., and Metge, D. (1997). Transport and recovery of bacteriophage PRD1 in a sand and gravel aquifer: Effect of sewage-derived organic matter. *Environmental Science & Technology*, 31(4):1163–1170.

Redman, J., Estes, M. K., and Grant, S. B. (2001a). Resolving macroscale and microscale heterogeneity in virus filtration. *Colloids and Surfaces A*, 191(1–2):57–70.

Redman, J., Grant, S. B., and Estes, M. K. (2001b). Pathogen filtration, heterogeneity, and the potable reuse of wastewater. *Environmental Science & Technology*, 35:1798–1805.

Reynolds, J. and Barrett, M. (2003). A review of the effects of sewer leakage on groundwater quality. *Water and Environment Journal*, 17:34–39.

Ryan, J., Elimelech, M., Ard, R., Harvey, R., and Johnson, P. (1999). Bacteriophage prd1 and silica colloid transport and recovery in an iron oxide-coated sand aquifer. *Environmental Science & Technology*, 33:63–73.

Ryan, J. N. and Elimelech, M. (1996). Colloid mobilization and transport in groundwater. *Colloids and surfaces A: Physicochemical and engineering aspects*, 107:1–56.

Sadeghi, G. (2012). *Effect of hydrochemical conditions in transport properties of viruses in groundwater*, volume 17. Utrecht University, Faculty of Geosciences, Department of Earth Sciences.

Sadeghi, G., Behrends, T., Schijven, J., and Hassanizadeh, S. M. (2012). *Effect of dissolved calcium on the removal of bacteriophage PRD1 during soil passage: The role of double-layer interactions*, volume 144. Elsevier.

Sadeghi, G., Schijven, J. F., Behrends, T., Hassanizadeh, S. M., and van Genuchten, M. (2013). Bacteriophage PRD1 batch experiments to study attachment, detachment and inactivation processes. *Journal of Contaminant Hydrology*, 152:12–17.

Schijven, J. (2001). Virus removal from groundwater by soil passage: modeling, field and laboratory experiments. Technical report, Ponsen and Looijen B.V., Wageningen.

Schijven, J. and Hassanizadeh, S. (2000). Removal of viruses by soil passage: Overview of modeling, processes, and parameters. *Critical Reviews in Environmental Science and Technology*, 30(1):49–127.

Schijven, J., Hassanizadeh, S., Dowd, S., and Pillai, S. (2000a). Modeling virus adsorption in batch and column experiments. *Quantitative Microbiology*, 2:5–20.

Schijven, J., Medema, G., Vogelaar, and Hassanizadeh, S. (2000b). Removal of microorganisms by deep well injection. *Journal of Contaminant Hydrology*, 44:301–327.

Shen, C., Huang, Y., Li, B., and Jin, Y. (2008). Effects of solution chemistry on straining of colloids in porous media under unfavorable conditions. *Water Resources Research*, 44:W05419.

Simoni, S. F., Bosma, T. N., Harms, H., and Zehnder, A. J. (2000). Bivalent cations increase both the subpopulation of adhering bacteria and their adhesion efficiency in sand columns. *Environmental science & technology*, 34(6):1011–1017.

Sinton, L., Finlay, R., Pang, L., and Scott, D. (1997). Transport of bacteria and bacteriophages in irrigated effluent into and through an alluvial gravel aquifer. *Water Air and Soil Pollution*, 98:17–42.

Tosco, T., Tiraferri, A., and Sethi, R. (2009). Ionic strength dependent transport of microparticles in saturated porous media: modeling mobilization and immobilization phenomena under transient chemical conditions. *Environmental Science & Technology*, 43(12):4425–4431.

Tufenkji, N. (2007). Modeling microbial transport in porous media: Traditional approaches and recent developments. *Advances in Water Resources*, 30:1455–1469.

Tufenkji, N. and Elimelech, M. (2004a). Correlation equation for prediciting singlecollector efficiency in physicochemical filtration in saturated porous media. *Environmental Science & Technology*, 38(2):529–536.

Tufenkji, N. and Elimelech, M. (2004b). Deviation from the classical colloid filtration theory in the presence of repulsive dlvo interactions. *Langmuir*, 20(25):10818–28.

Tufenkji, N. and Elimelech, M. (2005). Breakdown of colloid filtration theory: role of secondary energy minimum and surface charge heterogeneities. *Langmuir*, 21:841–852.

Tufenkji, N., Ryan, J., and Elimelech, M. (2002). The promise of bank filtration. *Environmental Science & Technology*, 36(21):422A–428A.

Yao, K. M., Habibian, M. T., and OMelia, C. (1971). Water and waste water filtration: concepts and applications. *Environmental Science & Technology*, 5:1105–1112.

Yates, M. and Yates, S. (1991). Modeling microbial transport in the subsurface: A mathematical discussion. In Hurst, C., editor, *Modeling the environmental fate of microorganisms*, pages 48–76. American Society for Microbiology, Washington, DC.

Yates, M., Yates, S., Wagner, J., and Gerba, C. (1987). Modeling virus survival and transport in the subsurface. *Journal of Contaminant Hydrology*, 1(3):329–345.

A Release Experiments

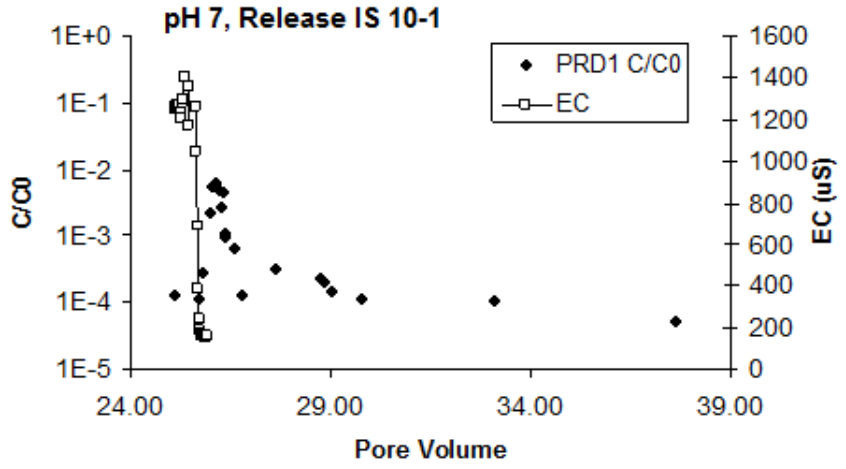

Figure A.1: Experiment 1 ($Ca^{2+} = 0$, pH = 7, IS = 10) with release (IS = 1) compared to EC breakthrough.

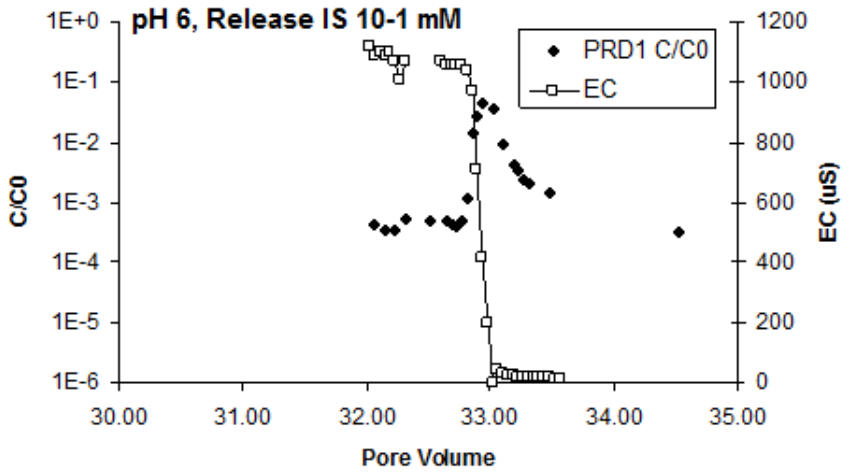

Figure A.2: Experiment 2 ($Ca^{2+} = 0$, pH = 6, IS = 10) with first release results and EC breakthrough.

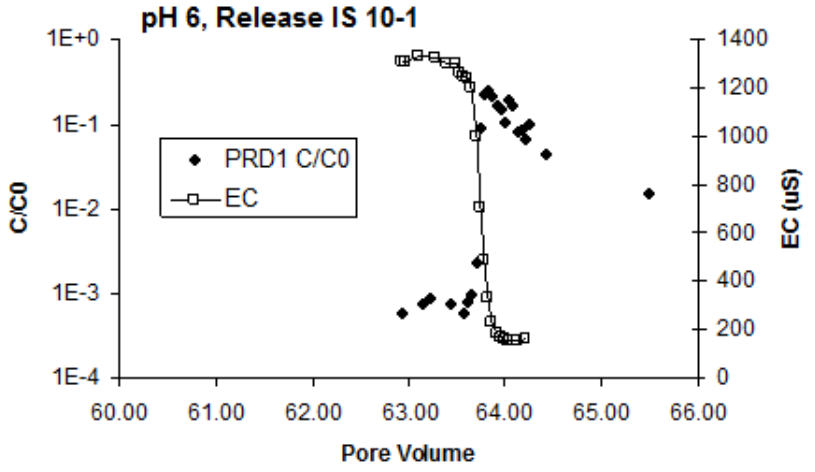

(a) EC breakthrough

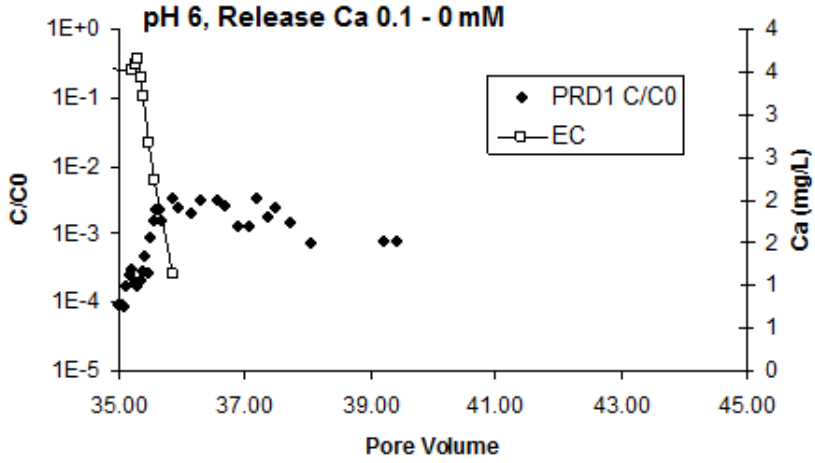

(b) Ca^{2+} concentration

Figure A.3: Experiment 6 ($Ca^{2+} = 0.1$ mM, pH = 6, IS = 10) release 1 and 2 results with respect to both (a) EC breakthrough and (b) Ca^{2+} concentration and PRD1 normalized concentration.

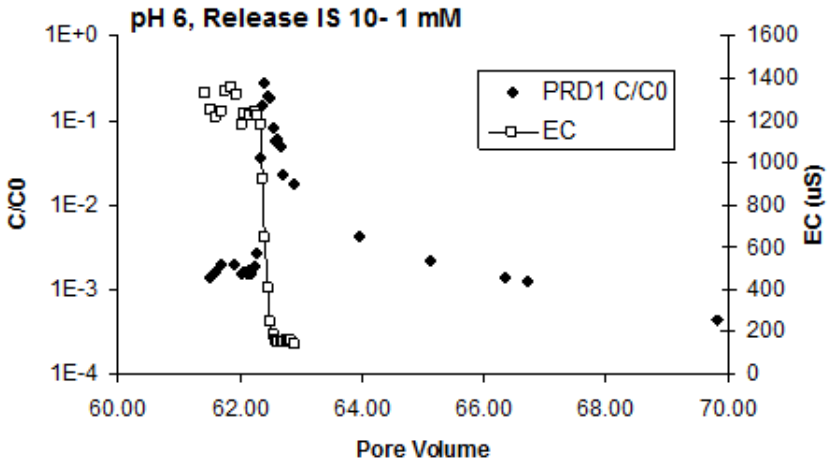

(a) EC breakthrough

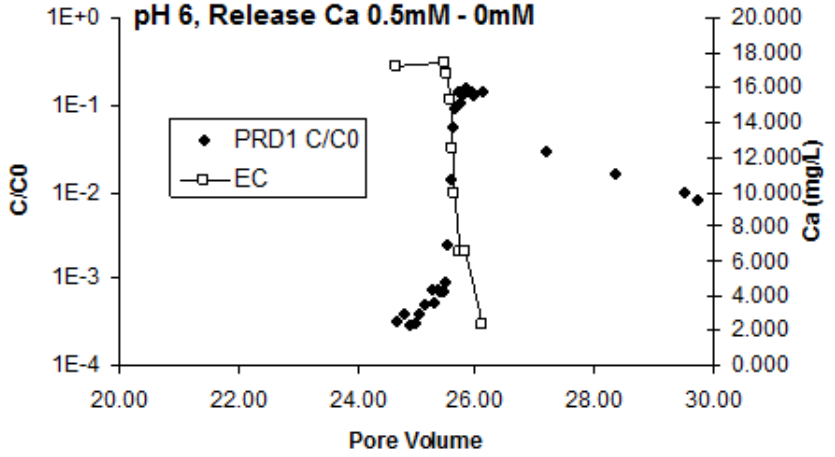

(b) Ca^{2+} concentration

Figure A.4: Experiment 5 (Ca^{2+} = 0.5, pH = 6, IS = 10) release 1 and 2 results with respect to both (a) EC breakthrough and (b) Ca^{2+} concentration and PRD1 normalized concentration.

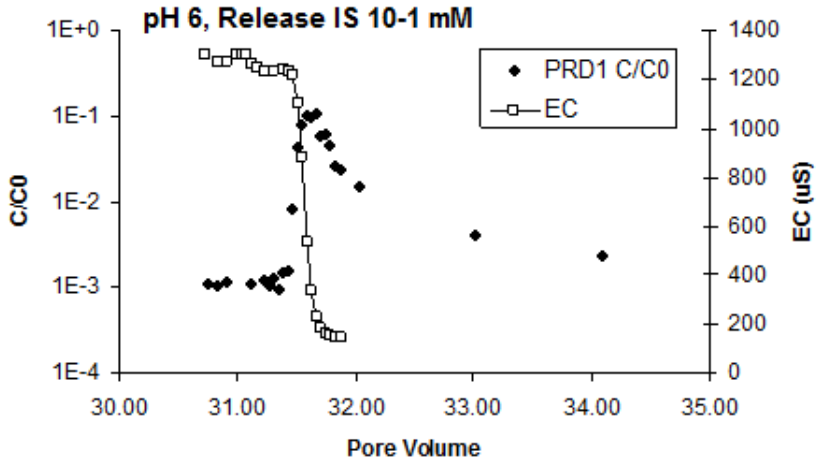

(a) EC breakthrough

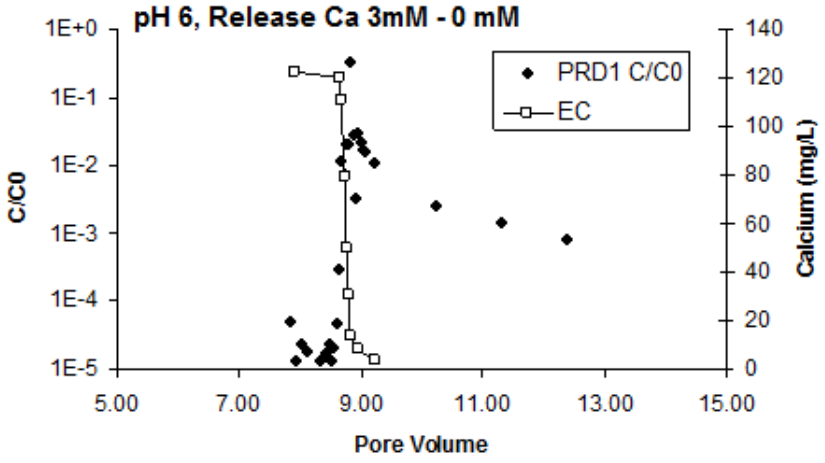

(b) Ca^{2+} Concentration

Figure A.5: Experiment 3 ($Ca^{2+} = 3$, pH = 6, IS = 10) with release 1 and 2 results with respect to both (a) EC breakthrough and (b) Ca^{2+} concentration and PRD1 normalized concentration.

B ICP Analysis

Tube	PV	120 (mg/L)	20 (mg/L)	4 (mg/L)
3	7.92	122.37	17.19	3.55
21	8.64	120.32	17.42	3.53
22	8.68	110.84	16.84	3.58
23	8.72	79.24	15.32	3.65
24	8.76	49.66	12.55	3.44
25	8.80	30.30	9.98	3.22
27	8.84	13.78	6.48	2.68
29	8.96	8.54	6.48	2.23
36	9.23	3.94	2.31	1.13

Table B.1: ICP Analysis of Ca^{2+} during first remobilization phase for experiments at 3 mM (120 mg/L), 0.5 mM (20 mg/L) and 0.1 mM (4 mg/L)